International Atomic Energy Agency

INDC(CCP)-289/L

INDC

INTERNATIONAL NUCLEAR DATA COMMITTEE

TRANSLATION OF SELECTED PAPERS PUBLISHED IN

NUCLEAR CONSTANTS, NO. 1, MOSCOW 1988

(Original Report in Russian was distributed as INDC(CCP)-288/G)

Translated by the IAEA

December 1988

IAEA NUCLEAR DATA SECTION, WAGRAMERSTRASSE 5, A-1400 VIENNA

INDC(CCP)-289/L

TRANSLATION OF SELECTED PAPERS PUBLISHED IN

NUCLEAR CONSTANTS, NO. 1, MOSCOW 1988

(Original Report in Russian was distributed as INDC(CCP)-288/G)

Translated by the IAEA

December 1988

Reproduced by the IAEA in Austria
December 1988

88-05778

Table of Contents

Part I

Part II

^{239}Pu NEUTRON CROSS-SECTIONS IN THE RESOLVED-RESONANCE REGION

A.A. Luk'yanov, V.V. Kolesov, S. Toshkov[*] and N. Yaneva[*]

ABSTRACT

The authors have determined the multi-level parameters for description of the total and fission cross-sections for ^{239}Pu in the resolved-resonance region up to 500 eV. A method has been developed for the construction of the elastic scattering and radiative capture resonance cross-sections using these parameters. The group-averaged cross-sections for experimental and evaluated data have been calculated in the energy region considered.

Multi-level analysis of the total and fission cross-sections

While there is a large volume of experimental data on the energy structure of the ^{239}Pu neutron cross-sections in the resonance region, only a few of the available data sets can be used in practice in the problem of multi-level parametrization of this structure. Here, apart from good experimental resolution in a relatively wide energy range, we also need a high accuracy of cross-section measurements, especially in the region of the interference minima, which are important particularly for multi-level description of the fission cross-section energy structure. To represent the ^{239}Pu resonance cross-sections, the evaluated data libraries at present generally use the measurement results of Blons, Derrien and Gwin [1-6] with subsequent corrections on the basis of the new data for the energy-averaged cross-sections [7-9]. These data in the region below 500 eV, where the resonances can be regarded as satisfactorily resolved, are analysed in the present paper.

The multi-level description of the cross-sections for fissionable nuclei, especially ^{239}Pu, was performed in several studies using various scheme of the resonance reaction theory [10]. Thus, the formalism of the R-matrix theory was used for this purpose in Refs [11-15] and the so-called Adler-Adler scheme - a simplified version of S-matrix parametrization - in Refs [16-19]. The present study also uses the Adler-Adler scheme to determine the consistent set of the corresponding resonance parameters for the combined analysis of the total and fission cross-sections in the whole region of resolved levels up to 500 eV. The resonance cross-sections constructed with

[*] Institute of Nuclear Research and Nuclear Power, Bulgarian Academy of Sciences, Sofia.

the parameters found by us reproduce all the observed characteristics of the cross-section energy structure in the region considered [20].

To describe the energy dependence of the cross-sections in the resolved region, we use the general expression for collision matrix elements $S^J(E)$ with the given value of total moment J and parity:

$$S^J_{nc}(E) = exp(-i\varphi_n)\left(\delta_{nc} + i\sum_k \frac{\Gamma^{1/2}_{kn}\Gamma^{1/2}_{kc}}{E_k - E}\right)exp(-i\varphi_c). \qquad (1)$$

The complex parameters $E_k = \mu_k - i\nu_k$ and $\Gamma^{1/2}_{kc}$ are assumed to be independent of energy, except for $\Gamma_{kn} \simeq \sqrt{E}$ [10, 16]. The total and fission cross-sections are expressed in terms of the elements of the S^J-matrix;

$$\sigma(E) = 2\pi\lambda^2 \sum_J g_J\left[1 - Re\, S^J_{nn}(E)\right];$$

$$\sigma_f(E) = \pi\lambda^2 \sum_J g_J \sum_{c(f)} \left|S^J_{nc}(E)\right|^2, \qquad (2)$$

where g_J is the spin factor and the sum over c(f) takes into account the possibility of several channels for the fission process [10]. Substituting expression (1) into (2) and considering the effective resonance broadening due to the thermal motion of the nuclei of the medium and the finiteness of the experimental resolution, we arrive at the well-known Adler-Adler formulae for the multi-level representation of the observed resonance cross-sections [10, 16]:

$$\sigma(E) = \sigma_p + \pi\lambda^2\sqrt{E}\sum_k\left[\frac{G^T_k}{\nu_k}\psi\left(\frac{\mu_k - E}{\nu_k}, \frac{\nu_k}{\Delta}\right) - \frac{H^T_k}{\nu_k}\chi\left(\frac{\mu_k - E}{\nu_k}, \frac{\nu_k}{\Delta}\right)\right]; \qquad (3)$$

$$\sigma_f(E) = \pi\lambda^2\sqrt{E}\sum_k\left[\frac{G^F_k}{\nu_k}\psi\left(\frac{\mu_k - E}{\nu_k}, \frac{\nu_k}{\Delta}\right) - \frac{H^F_k}{\nu_k}\chi\left(\frac{\mu_k - E}{\nu_k}, \frac{\nu_k}{\Delta}\right)\right]. \qquad (4)$$

here

$$\sigma_p = 4\pi\lambda^2 \sin^2\varphi_n - \qquad (5)$$

is the potential cross-section (phases φ_n are assumed to be independent of J); ψ and χ are the resonance form functions taking into account averaging over the Gauss distribution: $\Delta^2 = \Delta^2_R + \Delta^2_T$, where Δ_R is the width (dispersion) of the experimental resolution function and Δ_T the Doppler width [10]. The parameters in the analysis of experimental data are the values of μ_k and ν_k common to all cross-sections of the given element and also

$$G^T_k - iH^T_k = 2g_J exp(-2i\varphi_n)\Gamma_{kn}/\sqrt{E}; \qquad (6)$$

$$G^F_k - iH^F_k = \frac{2g_J}{\sqrt{E}}\sum_{c(f)}\sum_{k'(J)}(\Gamma_{kn}\Gamma^*_{k'n}\Gamma_{kc}\Gamma^*_{k'c})^{1/2}/(E^*_{k'} - E_k), \qquad (7)$$

The sum over $k'(J)$ relates here to resonances of one spin and parity value (in the case of ^{239}Pu, s-wave resonances with J equal to 1 and 0 correspond to the resolved region).

In order to determine the parameters of the scheme from the experimental data on the ^{239}Pu resonance cross-sections, we constructed a program of linear search with subsequent broadening of the energy region used in the analysis of Ref.[21]. As a result, we could obtain the consistent set of parameters μ_k, G^T_k, H^T_k, H^F_k, ν_k (Table 1), which enables us

Table 1. Parameters of the combined multi-level analysis of the ^{239}Pu cross-sections.

μ, eV	$G^T \cdot 10^6$, $eV^{1/2}$	$G^F \cdot 10^6$, $eV^{1/2}$	$H^T \cdot 10^6$, $eV^{1/2}$	$H^F \cdot 10^6$, $eV^{1/2}$	ν, MeV	J
-0,260	0,0	0,0	4I,454	3I.960	I00,0	0
0,260	I0,340	3.595	0,0	0,0	I00.0	0
0,299	2I4,292	I29,3I8	6,072	3,458	47.I	I
I,580	50,I07	22.I88	57,4I5	20,490	2250.0	0
7,807	4I4,603	230.I86	-7,488	-6,594	42.9	I
I0,920	830,202	623.722	50,632	5I,270	88,9	I
II,880	4I8,I44	I64,6I3	-32,I02	-33,35I	33.I	I
I4,30I	258,094	I6I,463	-32,I48	-37,I53	53.2	I
I4,66I	736,000	325,263	50,260	39,075	36.4	I
I5,4I7	282,I5I	253.I36	-I7,96I	-25.966	404,6	0
I7,633	638,244	290,233	I,877	-5,705	38.2	I
22,239	8I5,360	477,964	22,730	II,524	52.4	I
23,880	28,235	I4.379	-4,255	-4,6I6	45.8	I
26,230	448,8I7	225,867	2.595	-4,404	43.0	I
27,236	39,225	4,699	2.I50	-0,267	24.5	I
32,289	72,670	52,74I	2,05I	I.990	83.0	0
35,426	58,293	6,II0	0,057	-0.I07	I9.4	I
4I,375	884,634	7I,400	33,879	6,636	22.5	I
4I,626	299,937	I39,449	-I2,2[illegible]2	-8,862	50,6	I
44,436	I345,95I	I20,529	37,864	-2,660	25,8	I
47,559	369,974	324,595	26,475	I5,687	I40,6	0
49,648	240,744	239,689	I9,544	II,758	366,5	0
50,037	629,376	I38,I03	I0,879	-4,730	26,8	I
52,536	2000,650	270,773	7I,993	4,660	28.8	I
55,580	305,0I5	II5,950	-0,403	-I4,768	28,5	I
57,4I5	I492,228	I372,24I	622,323	522,352	465,9	0
59,I55	902,246	655,852	30,723	-2,483	69,3	I
63,03I	II3,379	7I,339	0,065	-I,884	49,4	I
63,603	977,862	948,770	-II80,I60	-948,770	35I0,9	0
65,454	7I5,369	538,243	2I0,550	3I8,9I0	I95,6	0
65,704	I666,989	593,2I0	I95.543	-22,5I4	33,6	I
74,028	569,493	263,456	-7I,893	-82,425	38,9	I
74,90I	34I4,305		23I,8I7	I02,635	93,0	I
78,940	I0,682	0,22	2,283	-0,369	62,6	I
8I,I29	255,598	I99,74I	398,05I	399,482	835,4	0
82,663	56,367	3,380	I,I55	-2,870	24,4	I
85,424	2832,952	2592,6I0	-344,838	-470,8I5	II65,0	0
85,488	I239,922	236,I2I	40,29I	-I8,I86	38,2	I
90,722	I746,850	269,058	86,667	-6,340	30,I	I
92,969	I00,498	9,284	-I,II0	-6,84I	20,7	I
95,374	296,672	88,270	27,I72	-5,397	38,9	I
96,653	528,546	489,535	-II5,832	-I05,788	73I,9	0
98,867	I538,524	I248,382	I48,6II	499,353	4652,0	0
I03,0I2	228,42I	47,755	I0,27I	-3,827	24,9	I
I05,3I3	652,249	69,742	29,43I	-I,963	29,9	I
I06,687	I253,704	465,I99	62,790	-30,667	36,4	I
II0,4I5	63,I45	26,277	2,044	-4,658	29,8	I
II3,960	20,939	I9,974	93,752	85,I56	9I9,I	0
II5,284	I8,394	0,562	-I9,604	-20,007	85,8	I
II6,062	475,96I	369,520	54,245	-7,643	I22,2	0
II8,840	22I2,866	906,462	93,086	-46,784	40,8	I
II9,22I	6I,349	30,I32	-22,II0	27,758	405,0	0
I2I,020	302,898	I46,495	-7,022	-22,402	23,9	I
I23,484	68,572	37,76I	-0,356	-I5,620	40,4	I
I26,234	208,270	46,890	I2,535	-I,894	I9,8	I
I27,569	62,8I3	I7,9I7	-I,585	-8,640	I8,5	I
I32,037	II02,596	I064,389	-I0I,929	-238,700	I574,8	0
I33,803	534,738	82,806	I8,5I0	-3,487	22,2	I
I35,230	I055,I6I	579,508	-672,458	-I49,806	7505,9	0

Table 1. (continued)

μ, eV	$G^T \cdot 10^6$, eV$^{1/2}$	$G^F \cdot 10^6$, eV$^{1/2}$	$H^T \cdot 10^6$, eV$^{1/2}$	$H^F \cdot 10^6$, eV$^{1/2}$	ν, MeV	J
I36,788	4I0,I32	279,598	I0,999	-3I,8II	50,3	I
I39,2I3	6,820	2,996	5,I35	0,999	25,0	I
I42,96I	372,204	242,I85	-8,405	-26,500	40,5	I
I43,476	508,I34	222,585	52,049	-3,239	42,0	I
I46,I36	I42,303	7I,500	52,I88	6I,I62	406,I	0
I46,266	650,I92	I07,874	7I,286	-27,690	I5,0	I
I48,293	42,9I5	24,470	-9,543	-20,200	47,2	I
I48,929	292,252	I59,793	-I03,458	26,965	2402,4	0
I49,453	I66,72I	6I,33I	I6,506	-I5,3I0	26,2	I
I56,989	208,3I0	I73,355	97,770	-92,532	80,4	0
I57,095	II88,507	599,223	-2I,580	46,766	442,6	0
I62,070	I3,630	2,650	-5,3I6	-I0,245	75,0	I
I64,566	3076,663	3I9,585	I90,575	-I4,709	40,8	I
I65,400	903,623	574,255	-290,I38	79,896	8836,3	0
I67,I36	68I,940	385,750	29,29I	-34,049	49,2	I
I70,532	70,762	57,526	-I5,050	0,282	I00,0	0
I7I,I00	237,479	94,866	-7,234	-II2,354	I500,0	0
I76,008	232,770	95,944	I2,430	-4,509	37,2	I
I77,252	380,248	53,809	22,398	-0,052	2I,4	I
I78,935	I33,438	35,279	7,033	I,274	25,I	I
I83,673	I73,243	63,I90	II,528	-I,255	20,0	I
I85,I32	742,568	544,294	-49,505	-83,7I7	I0II,0	0
I88,3I3	68,354	20,4I8	0,652	0,852	29,3	I
I90,665	I70,560	46,8I0	I3,438	3,995	26,3	I
I95,359	2020,036	I677,826	I78,2I7	99,27I	24I,5	0
I96,7I9	427,629	I62,895	55,I00	I9,705	40,4	I
I99,443	968,62I	523,756	43,033	-0,432	63,I	I
203,380	I44,977	6,872	I02,762	28,I69	46,I	I
203,964	2208,579	I697,9I9	-I24,I0I	-I49,806	275,4	0
207,4I3	676,5I4	75,326	44,263	-2,785	I5,6	I
207,880	I44,2I7	93,25I	-II4,844	-85,307	I000,0	0
2II,063	323,339	299,6I2	I83,027	I70,578	II54,9	0
2I3,235	38,633	I9,705	2I,069	I0,477	I04,3	0
2I6,582	620,049	86,743	27,964	-5,994	33,6	I
2I9,55I	305,I25	I00,204	-29,604	-I7,499	I5,0	I
220,273	797,542	207,043	-8,579	-23,243	59,3	I
223,2I6	304,975	37,923	2,752	-2,742	I5,7	I
224,930	I42,677	35,859	I0,406	9,473	I7,5	I
227,770	I308,645	9I8,809	46,334	99,87I	4500,0	0
227,940	I62,I89	67,825	I2,578	8,2I7	33,5	I
23I,433	I089,052	II7,7I0	97,968	9,7I4	23,2	I
232,588	24,720	22,I95	I8,I75	I4,38I	24,7	I
234,357	909,505	I83,572	80,982	0,I83	35,2	I
239,090	492,II6	I03,74I	27,288	-I0,I24	32,0	I
240,650	323,762	254,669	-265,443	-I84,942	4078,5	0
242,922	603,007	36I,628	44,873	I,6I9	58,2	I
247,637	I24,322	87,623	-33,352	-II,060	257,4	0
248,90I	I336,733	I37,637	79,992	II,2II	40,2	I
25I,272	2479,667	383,373	I80,962	-2,267	47,9	I
254,644	265,924	II6,3I2	9,I9I	5,874	42,I	I
256,I5I	56I,266	I5I,094	56,995	I9,687	5I,9	I
259,040	3,I62	3,I26	-8,466	-25,920	242,0	0
262,4I0	3708,40I	337I,56I	66,986	4,632	35I4,7	0
262,748	23I,9II	50,39I	57,06I	23,959	46,7	I
269,I50	I33,592	55,590	7,93I	I,I86	73,3	0
269,589	365,756	I64,232	27,802	6,967	30,5	I
272,686	238I,697	889,886	II3,980	-6I,892	6I,2	I
274,840	I2I3,695	II49,870	35I,354	227,I33	630,2	0
275,63I	I950,245	946,435	I06,3I5	-I9,II5	73,5	I
277,270	343,058	I59,793	456,694	483,000	2650,0	0
279,609	668,058	285,427	53,I39	-I,I33	43,3	0
282,970	2I79,I24	223,384	I73,084	-I6,473	42,7	I
288,040	895,686	769,570	94,448	38,435	3500,0	0
292,4II	33I,724	I58,439	I0,45I	-20,753	63,9	0
296,538	28I,033	III,00I	I4,979	-2,223	52,0	I
298,655	846,3I4	253,40I	79,983	I4,666	44,9	I
30I,888	I537,87I	70I,985	I22,368	-24,662	58,6	I
308,3I6	279,I29	22I,80I	-29,583	-37,89I	97,7	0
309,068	II2I,458	324,33I	I40,592	56,II6	47,4	I
3II,228	68,9I2	34,665	0,732	9,729	40I,0	0
3I3,692	I087,I6I	I87,798	89,560	I,52I	39,9	I
3I6,729	428,225	I59,II3	46,I09	-0,937	59,9	I
32I,850	326,689	325,577	-I7,502	I06,909	4406,9	0
323,447	I569,544	369,287	92,275	I,024	84,0	0
325,38I	679,309	25I,202	53,42I	-2,260	65,4	I

Table 1. (continued)

μ, eV	$G^T \cdot 10^6$, eV$^{1/2}$	$G^F \cdot 10^6$, eV$^{1/2}$	$H^T \cdot 10^6$, eV$^{1/2}$	$H^F \cdot 10^6$, eV$^{1/2}$	ν, MeV	J
329,750	337,833	I92,732	-4I,404	-30,643	2I09,5	0
333,990	4I7,463	7I,703	36,020	8,396	4I,3	I
336,0I4	II39,586	262,749	83,993	2,320	45,4	I
338,037	6II,05I	I02,853	4I,524	-4,982	42,0	I
339,336	266,902	I05,494	I0,560	-6,492	59,2	0
343,266	II86,893	356,I27	97,85I	-I7,427	54,0	I
346,557	39I,278	3I6,354	40,55I	44,942	757,5	0
350,399	I592,396	630,963	I32,353	-22,2I7	59,3	I
352,9I5	305,720	96,456	20,029	-0,630	54,5	I
355,050	33,I84	I9,542	-6,347	-8,859	8I,3	0
357,970	256,I02	I9I,942	-I5I,272	-32,094	3000,0	0
360,II5	96,438	50,938	-7,8I2	-II,204	93,5	0
36I,380	26,896	I7,55I	-3,625	-5,55I	I07,2	0
366,I00	246,359	242,685	-296,442	-I30,503	2500,0	0
368,609	64,I85	24,968	-46,867	-I4,609	378,5	0
370,457	I8I,275	I4,24I	-2I,504	-I0,288	45,3	I
37I,820	I260,358	979,40I	-44,539	-I64,04I	2289,8	0
375,I09	204,I62	4I,003	24,646	6,634	38,7	0
377,I82	I76,68I	79,796	25,030	3,703	I02,4	0
378,072	74,899	I0,278	3I,576	I6,798	79,0	0
382,593	I9,250	4,994	-6,445	-2,760	I5,4	I
383,765	9II,057	I79,767	-37,266	-2,397	4298,2	0
384,35I	423,823	238,627	45,546	2,77I	65,6	I
389,595	I02,657	I9,853	I6,682	8,806	49,0	I
39I,605	7I,686	33,475	II,957	-0,999	76,3	0
394,543	466,683	24I,4I6	2I,I74	-29,45I	65,6	I
397,029	I67,68I	I08,59I	7,350	-I4,729	85,9	0
40I,250	I8I,453	39,948	-I26,897	-69,909	I000,0	0
40I,690	I322,665	994,248	I3I,938	-40,956	II0,0	I
404,320	I509,38I	827,773	2I2,4I5	-53,52I	77,5	I
404,900	323,35I	I79,844	I9,207	I39,908	I000,0	0
406,I40	II3,904	I5,439	67,224	3I,224	I60,0	0
407,027	45,I49	37,95I	38,328	0,999	I65,0	0
408,830	87,982	25,445	25,315	II,365	75,0	I
4I2,4I0	6I7,522	3I4,554	68,540	-I4,432	72,5	I
4I5,780	228,999	37,934	I5,I65	-5,I60	76,0	I
4I7,720	I26,458	56,457	9,774	-25,467	I33,5	0
4I9,940	4I7,865	225,072	2I,374	-33,52I	69,5	I
425,700	II,079	2,497	I2,320	-I,725	7I,0	I
426,450	600,500	499,353	-3I3,370	-33I,570	3500,0	0
429,720	276,725	26I,II3	-0,7I0	-30,0I7	390,0	0
43I,370	588,787	5I8,783	-38,039	-33,438	I750,0	0
432,8I0	57,I24	20,063	43,0I9	36,675	I70,0	0
437,885	I8I,I26	44,723	-I2,400	-0,999	4I,6	I
438,964	2I7,983	33,423	-44,663	-I0,278	69,I	I
439,895	I75,720	29,96I	60,446	36,952	957,2	0
442,5I5	508,57I	406,5I3	75,II8	20,646	238,3	0
450,0II	75,508	47,I78	-33,090	-34,7I6	I25,3	0
45I,483	864,368	70,400	54,9I6	-8,5I4	55,I	I
455,736	9,90I	8,988	I889,750	II26,220	20I,5	0
455,764	I840,236	II78,472	-I863,532	-I292,055	320,0	0
457,497	588,666	499,353	-5,I84	-I2,284	2I5,8	0
458,906	352,704	I74,56I	68,I07	57,332	98,4	I
46I,454	237,534	I66,685	-I6,390	-3I,653	I99,9	0
462,509	74,004	52,809	89,626	63,245	302,I	0
468,34I	370,695	320,447	-43,263	-I26,399	I067,3	0
469,534	903,427	90I,83I	30I,955	359,534	2848,9	0
473,249	269,603	46,589	I0,4I6	-24,968	38,0	I
475,422	288,454	259,663	47,675	86,69I	389,6	0
477,050	I04,803	7,57I	34,003	47,938	I002,2	0
479,609	I3,564	9,987	-9,002	-I2,234	I27,4	0
484,30I	I73,I76	34,858	9,649	2,999	63,6	I
487,440	I27,087	I24,838	-44,78I	-80,590	I76,2	0
487,984	353,9I8	3I0,238	45,536	63,283	293,9	0
490,874	94I,324	684,II3	42,960	49,935	II48,9	0
494,263	334,I09	22I,658	I5,378	I2,753	97,4	I
495,794	48,980	5,789	6,I33	9,987	I02,3	0
500,677	25I,773	I39,8I9	2,578	8,533	60,8	I
502,994	7II,075	438,036	II3,969	72,282	98,3	I
506,I3I	I7,497	4,494	-I7,I00	-4,994	98,6	0
508,370	2,963	2,896	-28,790	28,348	346,3	0
509,890	3469,086	599,223	28I,464	-30,398	I30,7	0
5II,670	689,847	47I,675	-339,987	-257,939	I700,0	0
5I5,3I0	74,628	52,87I	-I8,I59	-I,0I4	24I,2	0

Table 1. (continued)

μ, eV	$G^T \cdot 10^6$, eV$^{1/2}$	$G^F \cdot 10^6$, eV$^{1/2}$	$H^T \cdot 10^6$, eV$^{1/2}$	$H^F \cdot 10^6$, eV$^{1/2}$	ν, MeV	J
516,720	35,653	35,454	-3,159	1,997	160,9	0
518,130	72,807	17,940	-4,661	16,650	218,8	0
520,401	906,819	362,349	46,014	-38,381	83,2	0
524,360	2053,283	382,787	257,619	8,948	45,5	1
525,642	6139,813	4993,523	-351,683	-588,712	5583,2	0
526,150	33,011	9,987	36,569	85,822	47,2	1
527,530	34,663	9,987	31,493	51,007	33,9	1
530,730	3081,960	756,912	133,752	-200,268	77,2	0
596,859	119,267	113,829	541,737	285,164	1374,8	0
596,905	2017,571	1353,805	-1824,245	-635,841	7527,8	0

Table 2. Values of the average ^{239}Pu fission cross-sections in specific energy intervals.

Energy, eV	$\bar{\sigma}_f = \frac{1}{\Delta E}\int_{\Delta E} \sigma_f(E)dE$						
	Gwin, 1976 [3]	Gwin, 1984 [7]	Weston 1984 1980 [8]	Wagemans, 1980 [9]	ENDF/B-IV*	Kon'shin, 1982 [5]*	Present work
6-9	60,7	59,6±0,6	-	60,6	60,9	61,4	59,8
9-12,6	137,5	140,1±1,3	-	138,4	139,7	135,9	137,5
12,6-20	73,4	70,7±0,7	-	73,8	73,9	66,7	72,5
20-24,7	47,7	46,2±0,6	-	47,5	47,7	43,9	46,6
50-100	56,96	-	56,56	57,4	56,9	60,75	55,7
100-200	17,96±0,04	-	17,98±0,03	18,9	18,4	19,22	18,7
200-300	17,90±0,05	-	17,23±0,04	17,9	17,7	17,69	17,9
300-400	8,48±0,03	-	8,064±0,022	—	—	9,43	9,1
0,0253	741,6	-	741,7	741,9	741,7	741,7	741,6

* Calculated from the file.

Table 3. Values of the average neutron radiative capture cross-sections for ^{239}Pu in specific energy intervals.

Energy, eV	$\bar{\sigma}_c = \frac{1}{\Delta E}\int_{\Delta E} \sigma_c(E)dE$			
	Gwin, 1976 [3]	ENDF/B-IV*	Kon'shin, 1982 [5]*	Present work
6-9	51,3	51,0	44,7	45,2
9-12,6	75,3	75,8	67,0	74,7
12,6-20	61,7	58,1	58,1	59,1
20-24,7	37,4	32,0	30,8	30,6
50-100	35,88	36,3	35,25	36,7
100-200	15,70	17,1	15,02	16,3
200-300	16,79	17,5	14,48	16,1
300-400	9,83	-	8,54	9,5
0,0253	271,3	270,2	271,3	271,3

* Calculated from the file.

Table 4.

Average vales of $\bar{\alpha}=\bar{\sigma}_c/\bar{\sigma}_f$ for ^{239}Pu in specific energy intervals

Energy, eV	$\bar{\alpha}=\bar{\sigma}_c/\bar{\sigma}_f$			
	Gwin, I976 [3]	ENDF/B-IV*	Kon'shin I982 [5]*	Present work
6-9	0,85	0,83	0,73	0,76
9-I2,6	0,55	0,54	0,49	0,54
I2,6-20	0,84	0,79	0,87	0,82
20-24,7	0,78	0,67	0,70	0,66
50-I00	0,63	0,64	0,58	0,66
I00-200	0.87±0,0I5	0,93	0,78	0,87
200-300	0,94±0,0I	0,99	0,82	0,90
300-400	I,I6±0,0I4	-	0,9I	I,04

* Calculated from file.

with the appropriate choice of Δ to reproduce by formulae (3) and (4) virtually all the observed characteristics of the energy dependence of σ(E) and of $\sigma_f(E)$ right up to 500 eV [20].

Parameters of the elastic scattering and radiative capture cross-sections

The analysis of the total cross-section (3) for a particular spin identification of resonance enables us to find not only parameters G_k^T and H_k^T but also neutron widths Γ_{kn} (6). Using these values, we can directly construct two more cross-sections determined by the diagonal elements of the S^J-matrix (1). These are the neutron absorption cross-sections

$$\sigma_a(E) = \pi\lambda^2 \sum_J g_J \left[1 - |S_{nn}^J(E)|^2\right] =$$
$$= \pi\lambda^2 \sqrt{E} \sum_k \left[\frac{G_k^a}{\nu_k}\,\psi\!\left(\frac{\mu_k - E}{\nu_k}, \frac{\nu_k}{\Delta}\right) - \frac{H_k^a}{\nu_k}\,\chi\!\left(\frac{\mu_k - E}{\nu_k}, \frac{\nu_k}{\Delta}\right)\right], \qquad (8)$$

where

$$G_k^a - iH_k^a = (G_k^T - iH_k^T)\exp(2i\varphi_n) -$$
$$- i\frac{\sqrt{E}}{2g_J}\sum_{k'(J)} \frac{(G_k^T G_{k'}^T + H_k^T H_{k'}^T) - i(H_k^T G_{k'}^T - H_{k'}^T G_k^T)}{\mu_{k'} - \mu_k + i(\nu_k + \nu_{k'})} \qquad (9)$$

and the elastic scattering cross-section

$$\sigma_n(E) = \sigma(E) - \sigma_a(E) . \tag{10}$$

Using the found values of parameters G_k^T and H_k^T (see Table 1) for each possible value of spins J, we can find the absorption cross-section parameters G_k^a and H_k^a (9) and construct cross-sections $\sigma_a(E)$ (8) for Δ corresponding to the measurement results given in Ref.[3].

For neutron elastic scattering cross-section $\sigma_n(E)$ (10) there are virtually no direct experimental data on energy dependence in the resonance region, and we give only the calculated dependence $\sigma_n(E)$ for T = 300 K. Thus, $\sigma_a(E)$ and $\sigma_n(E)$ obtained from the total cross-section parameters contain all the characteristic features of the resonance structure in the region under consideration, the errors of reproduction of these features being of the same order as in the case of the total cross-sections measured with the best resolution [19].

It is obvious that, constructing the absorption cross-section and having reliable fission cross-sections $\sigma_f(E)$, we can also determine the resonance dependence of the radiative captive cross-section with the corresponding accuracy:

$$\sigma_c(E) = \sigma_a(E) - \sigma_f(E) = \pi \lambda^2 \sqrt{E} \sum_k \left[\frac{G_k^c}{\nu_k} \psi\left(\frac{\mu_k - E}{\nu_k}, \frac{\nu_k}{\Delta}\right) - \frac{H_k^c}{\nu_k} \chi\left(\frac{\mu_k - E}{\nu_k}, \frac{\nu_k}{\Delta}\right)\right] \tag{11}$$

with $G_k^c = G_k^a - G_K^F$, $H_k^c = H_k^a - H_k^F$ [22, 23]. The available experimental data [3] agree qualitatively with the results of our calculation of $G_c(E)$ (11). It is important that in this method of construction there are possibilities of correcting the total and fission cross-section parameters (see Table 1) and of more reliably determining the resonance spins. The most interesting are the regions near some interference minima, where the use of not sufficiently accurate total and fission cross-section data may lead to a discrepancy of results for our scheme (11). This can serve as an indication of the nature of errors in experimental data.

Comparison with integral data

The fission cross-section resonance parameters given in Table 1 were normalized to the last evaluation of σ_f = 748.1 b for 0.0253 eV

(σ_c = 269.3 b) [24]. The group-averaged fission and neutron-radiative-capture cross-sections and $\bar{\alpha} = \bar{\sigma}_c/\bar{\sigma}_f$ were compared with the available experimental data [3, 7-9] and contemporary evaluations (Tables 2-4). Here the normalization of the fission cross-section was taken to be the same as in Ref.[3].

From a detailed and consistent analysis of the whole set of ^{239}Pu resonance cross-sections in the proposed multi-level parametrization scheme we can draw specific conclusions regarding the degree of accuracy and consistency of the available experimental data. The differences from experiment and also the possible inconsistency of the different experiments obviously point to the need for further studies on the cross-sections both in direct measurements and in measurements of transmissions and self-indication cross-sections for relatively thick samples [25]. By refining these data with broadening of the range of the target thicknesses used it will be possible to make a further correction of the resonance parameters (mainly H_k^F and H_k^T) sensitive to the minima in the cross-sections.

A unified approach to the description of all cross-sections in the resolved region involving the direct use of the property of unitarity of the S^J-matrix (1) gives a useful interrelationship between the parameters of the different cross-sections, which can be used ultimately to solve the problem of unambiguous description of the resonance cross-sections. The scheme can be applied to other fissionable nuclei with specific resonance spins.

REFERENCES

[5] ANTSIPOV, G.V., KON'SHIN, V.A., SUKHOVITSKIJ, E.Sh., et al., Nuclear Data for Plutonium Isotopes, Nauka i Tekhnika, Minsk (1982) 168 (in Russian).

[6] ABAGYAN, L.P., BAZAZYANTS, N.O., NILOLAEV, M.N., TSIBULYA, A.M., Group Constants for Calculation of Reactors and Protection, Ehnergoizdat, Moscow (1981) (in Russian).

[10] LUK'YANOV, A.A., Neutron Cross-section Structure, Atomizdat, Moscow (1978) (in Russian).

[13] KIRPICHNIKOV, I.V., IGNAT'EV, K.G., SUKHORUCHKIN, S.I., "Interference effects in fission cross-sections", At. Ehnerg. 16 3 (1964) 211-218.

[18] TOSHKOV, S., Multi-level Analysis of the ^{239}Pu Fission Cross-section. Author's abstract of the thesis for the degree of Candidate of Physical Sciences, Sofia (1980) (in Russian).

[20] KOLESOV, V.V., LUK'YANOV, A.A., The Parameters of Multi-level Analysis of ^{239}Pu Cross-sections in the Resonance Region. Report FEhI-1404, Obninsk (1983) (in Russian).

[21] KOLESOV, V.V., "A program for multi-level analysis of resonance cross-sections" in: Problems of Atomic Science and Technology. Ser. Nuclear Constants No. 3(38) (1980) 17-20 (in Russian).

[22] KOLESOV, V.V., LUK'YANOV, A.A., "The ^{239}Pu neutron absorption cross-section in resonance region", At. Ehnerg. 58 3 (1985) 197-198.

ELASTIC AND QUASI-ELASTIC NUCLEON SCATTERING ON VANADIUM

N.N. Titarenko, A.G. Isakov and E.O. Rudenskaya

ABSTRACT

A unified set of the neutron optical potential parameters for the ^{51}V nucleus is sought in the 10 keV-32 MeV region so as to obtain a good agreement with all the available data. These include the neutron strength function and elastic scattering data as well as the neutron total cross-section and (p,n) isobaric analogue state quasi-elastic scattering data.

The optical model is used to analyse the elastic scattering of the simple and compound particles on nuclei in a wide energy range and forms the basis of many approaches describing more complex processes: inelastic scattering, charge exchange, stripping, pickup etc. [1]. It is of great practical value in the evaluations of nuclear data for reactor physics calculations.

The comparison of neutron and proton experimental data is of basic interest in the parametrization of the optical model potential. The parameters of the neutron optical potential at low energies can be found with the use experimental values of the s- and p-neutrons strength functions, potential scattering radii R' and total neutron cross-sections σ_t. The parameters of the proton optical potential are found usually from the experimental distributions at proton energies above the Coulomb barrier with the use of the differential cross-sections and by analysing elastic scattering. In the energy region near the Coulomb barrier and below the situation is complicated by the fact that either experimental data on the total cross-sections for the (p,n) reaction or the relatively non-informative differential cross-sections are used in the search for the optical potential parameters. From this standpoint, neutron elastic scattering at low energies is a finer instrument of study of the nuclear field.

According to the Lane model [2-5], the optical potential of nucleon elastic scattering on nuclei with a neutron excess contains an isovector component; it can be written in the charge-invariant form

$$U(r) = U_0(r) + 4U_1(r)(\vec{t}\,\vec{T})/A \,, \qquad (1)$$

where U_0, U_1 are the amplitudes of the isoscalar and isovector components of interaction; $\vec{t}$, $\vec{T}$ are the isospin of the scattered particle and target nucleus, respectively. In this model the cross-section of neutron and proton elastic scattering on the nucleus will be defined by the potentials

$$U_{nA} = U_0(\tau) - U_0'(E_n) + \varepsilon U_1(E_n); \tag{2}$$
$$U_{pA} = U_0(\tau) - U_0'(E_p) - \varepsilon U_1(E_p) + \Delta U_c . \tag{3}$$

Here $\varepsilon = (N-Z)/A$ is the coefficient of isotopic symmetry of the nucleus, where N,Z are the number of neutrons and protons of the target nucleus, $A = N + Z$. The proton optical potential (3) differs from the neutron optical potential (2) not only by the value and sign of the isovector component but also by the presence of the Coulomb correction ΔU_c in the optical potential due to the energy dependence of the nuclear potential in the presence of an electrostatic field.

The nucleon-nucleus optical potential in the charge exchange form (1) gives a simple interpretation of the (p,n) reaction which takes place with excitation of the isobaric analogue ground state [(p,n)IAS] and regards it as a quasi-elastic scattering process. It is assumed that in the (p,n)IAS reaction the neutron of the target nucleus is replaced directly by the proton, the residual nucleus being the isobaric analogue of the target nucleus. The quasi-elastic scattering cross-section is determined in the Lane model by the isovector component of the optical potential $U_{pn}(\tau) = 4U_1(\vec{t}\vec{T})/A = 2U_1\sqrt{N-Z}/A$.

As a result, the optical potential in form (1) without introduction of additional parameters describes in a unified manner the elastic scattering of protons and neutrons on nuclei and also the (p,n)IAS reaction.

The isovector part $U_1(\tau)$ of the optical potential can be determined from the difference between the neutron (2) and proton (3) potentials. However, it is very difficult to use this approach in practice to extract information on the energy dependence of the isovector part of the optical potential. The most direct means of studying $U_1(\tau)$ is to analyse the (p,n)IAS reaction [5-7]. The comparison of the calculations of this reaction with experimental data show [8-14], that, regardless of the type of interaction, the best agreement with experiment is obtained in the case of complex potential U_1 with a real volume form factor and an imaginary surface form factor. The cross-section of the (p,n)IAS reaction is very sensitive to the selection of parameters of the imaginary component of interaction.

In the present study we seek the parameters of the nucleon potential for the ^{51}V nucleus, which is a magic nucleus with respect to the number of neutrons, and this ensures the validity of using spherical optics. For this isotope a lot of experimental data are available on the (p,n)IAS reaction [8, 9] and on the elastic scattering of protons [15, 16] and neutrons [17-23]. The purpose of the study is to search for the nuclear optical potential parameters for ^{51}V and to verify the reliability of describing the experimental data in a wide kinematic range within the framework of the consequent Lane model.

Vanadium is an important material for fusion research. It is a component of reactor structural materials. From this standpoint, it is necessary to know the exact interaction of nucleons with this element.

The optical model of elastic scattering of particles with an arbitrary spin and charge

We shall describe the scattering of a particle of mass $\tilde{m}_a$, charge z_a, spin s_a and energy E_L on a spherical spinless nucleus of mass M and charge Z within the framework of the optical model by the complex local optical potential $V_{\ell j}(r)$. After separation of the variables in the complete Schroedinger equation, we obtain a radial equation for each value of orbital moment ℓ and total spin of the particle $\vec{j} = \vec{\ell} + \vec{s}_a$ [1, 24-27]:

$$\left[\frac{d^2}{dr^2} - \ell(\ell+1)/r^2 + k^2 - \frac{2\tilde{\mu}}{\hbar^2} V_{\ell j}(r)\right] \chi_{\ell j}(r) = 0 . \qquad (4)$$

Here $k = \sqrt{2\tilde{\mu}E/\hbar^2}$ is the wave number, where $\tilde{\mu} = \tilde{m}_o M/(\tilde{m}_o + M)$ is the reduced mass of the particle; $E = E_L M \times \tilde{m}_a + M$ is the energy of the particle in the centre-of-mass system; E_L is the energy of the particle in the laboratory system. The radial wave function $\chi_{\ell j}(r)$ satisfies the boundary conditions

$$\begin{aligned} &\chi_{\ell j}(r) \underset{r\to 0}{\Longrightarrow} \rho^{\ell+1} \quad (\text{for } \rho = kr); \\ &\chi_{\ell j}(r) \underset{r\to\infty}{\Longrightarrow} \frac{i}{2}\left\{G_\ell(\rho) - iF_\ell(\rho) - S_{\ell j}\left[G_\ell(\rho) + iF_\ell(\rho)\right]\right\} \exp\left[i(\sigma_\ell - \sigma_0)\right], \end{aligned} \qquad (5)$$

where functions $G_\ell(\rho)$ and $F_\ell(\rho)$ are, respectively, the irregular and regular solutions of the homogeneous Schroedinger equation for the Coulomb potential in the absence of nuclear interaction (Coulomb functions, σ_ℓ is their phase). In the case of neutron scattering, these functions are connected by simple relations with the spherical Bessel and Neumann functions having a half-integer index [28].

Calculations by the optical model mostly use the sphero-symmetric complex potential $V_{\ell j}(r)$ of the general form:

$$V_{\ell j}(r) = V_C(r) - V_R f_R(r) + 2\gamma V_{so} \frac{1}{r}\frac{d}{dr} f_{so}(r) - i\left[W_v f_v(r) - 4a_d W_d \frac{d}{dr} f_d(r)\right], \qquad (6)$$

where

$$\gamma = \left[j(j+1) - \ell(\ell+1) - s_a(s_a+1)\right], \quad f_i(r) = \left[1 + \exp\left(\frac{r - R_i}{a_i}\right)\right]^{-1} \qquad (7)$$

and all the dynamic parameters (V_R, V_{so}, W_v, W_d) are positive. The potential $V_c(r)$ of the Coulomb interaction of the scattered particle with the nucleus is approximated by the potential of a uniformly charged sphere of radius R_c.

At low energies of scattered neutrons the basic experimental data are the total neutron interaction cross-sections σ_t in the whole energy range, the strength functions of the s- and p-neutrons (S_0 and S_1) and the potential scattering radius R' determined at low neutron scattering energies (less than 100 keV). The potential scattering radius is connected with the integral potential elastic scattering cross-section by the relation $\sigma_{e\ell} = 4\pi R'^2$.

The procedure used most often to search for the optical potential parameters is that of automatic search from experimental data using the χ^2-criterion:

$$\chi^2 = \frac{1}{N_x}\sum_{i=1}^{N_x}\left(\frac{\sigma_T^i - \sigma_{exp}^i}{\Delta\sigma_{exp}^i}\right)^2 , \qquad (8)$$

where N_x is the number of experimental points, which are used for the search; σ_T^i, σ_{exp}^i, $\Delta\sigma_{exp}^i$ are the theoretical and experimental values of the cross-sections and the experimental error, respectively. By minimization of functional χ_2 in relation to the variable parameters of the model, their optimal set is determined.

Practical calculations by the optical model showed that determination of the potential from experimental data was not an unambiguous problem. The same cross-section can be described by several potentials whose parameters can differ substantially from each other. As was shown within the framework of the convolution model [1], the additional criteria for selection of parameters are the values of the volume integrals over the potential per nucleon of the nucleus and the root-mean-square radii.

If we take the radial dependence of the form factors of the volume and surface potentials in the Woods-Saxon form (6), (7), the interrelationship between the dynamic and geometric parameters for the real and imaginary components of the optical potential is determined by

$$(I/A)_R = (4\pi/3)\, r_R^3 V_R \left[1 + (\pi a_R/R_R)^2\right] ;$$
$$(I/A)_d = (16\pi R_d^2/A)\, a_d W_d \left[1 + \tfrac{1}{3}(\pi a_d/R_d)^2\right] , \tag{8A}$$

where $R_i = r_i A^{1/3}$. The sets of the optical model parameters with identical values of integrals $(I/A)_R$ and $(I/A)_d$ give a virtually equivalent description of experimental data. The root-mean-square radii of the above potential components will be determined by

$$\langle r_R^2 \rangle = \tfrac{3}{5}\left(R_R^2 + \tfrac{7}{3}\pi^2 a_R^2\right); \langle r_d^2 \rangle = R_d^2 + \tfrac{5}{3}\pi^2 a_d^2 .$$

Description of quasi-elastic scattering by the distorted wave method

The differential and integral cross-sections of the $^{51}V(p,n)$ reaction with excitation of the analogue ground state of the ^{51}Cr nucleus are calculated a first Born approximation of the distorted wave method by the VAR-82 program [26], in which the following relation is used to calculate the cross-section of the process in the general case

$$\frac{d\sigma}{d\Omega}(\theta) = \frac{2J_B+1}{4\pi E_\alpha E_\beta (2s_\alpha+1)(2J_A+1)} \left(\frac{k_B}{k_A}\right)\left(\frac{\tilde{M}_B}{\tilde{M}_A}\right)^2 \sum_{J_m \mu_a \mu_\beta} \left| \sum_{LS} \tilde{\beta}^{LSJ}_{m\mu_a\mu_\beta}(\theta) \right|^2 . \tag{9}$$

Here the reduced partial amplitude is determined by the expression

$$\tilde{\beta}^{LSJ}_{m\mu_a\mu_\beta}(\theta) = \sum_{L_a J_a L_\beta J_\beta} \Gamma^{LSJm\mu_a\mu_\beta}_{L_a J_a L_\beta J_\beta} P_{Lm}(\cos\theta) \tilde{f}^{LSJ}_{L_a J_a L_\beta J_\beta} (-1)^{2s_a+2s_\beta+S-J_a-J_\beta-J} \tag{10}$$

and the following notation of the radial integral is introduced

$$\tilde{f}^{LSJ}_{L_a J_a L_\beta J_\beta} = \int_0^\infty \chi_{L_a J_a}(k_\alpha r) G^T_{LSJ}(r) \chi_{L_\beta J_\beta}\left(k_\beta \frac{\tilde{M}_A}{\tilde{M}_B} r\right) dr . \tag{11}$$

The determination of the matrix of algebraic coefficients Γ is given in Ref.[26]. In relations (9)-(11) m_a, z_a, s_a, t_a are, respectively, the mass, charge, spin and isospin of the scattered particle and M_A, Z_A, J_A, T_A are the corresponding characteristics of the target nucleus. The final state of the system is characterized by the similar parameters $\tilde{m}_b$, z_b, s_b, t_b, $\tilde{M}_B$, Z_B, J_B, T_B. The program uses the multipole expansion of the interaction potential V over total spin J, isospin T, orbital moment L and spin s transmitted to the nucleus:

$$\vec{J} = \vec{J}_B - \vec{J}_A; \quad \vec{S} = \vec{s}_a - \vec{s}_b; \quad \vec{L} = \vec{J} - \vec{S}; \quad \vec{T} = \vec{T}_B - \vec{T}_A. \tag{12}$$

The procedure for calculating the amplitude and reaction cross-section by the distorted wave method is as follows. The interaction of the initial and final particles with nuclei is described within the framework of the optical model of elastic scattering on the complex potential of general form (5). For the input and output potentials the partial distorted waves waves $\chi_{L_a J_a}(k_a r)$ and $\chi_{L_b J_b}[k_b r(\tilde{M}_A/\tilde{M}_B)]$, needed for calculation of the radial integral (11) are found by numerically solving the radial Schroedinger equation (4). During its calculation it is necessary to know the structure of the form factor of interaction $G^T_{LSJ}(r)$. It has been shown in Ref.[26] that in quasi-elastic scattering all quantum numbers of the system, except the isospin projection, remain unchanged during charge exchange and that the form factor of interaction can be written in the form

$$G^T_{LSJ}(r) = G^1_{000}(r) = -4\sqrt{\pi(2s_a+1)(N-Z)}\,U_1(r)/A. \tag{13}$$

<u>Search for the neutron optical potential parameters</u>

In selecting the optical potential geometry the parameters from global systematics [29-31] and so on were taken as the starting values. A preliminary analysis of the experimental data showed that these were reproduced best with the optical potential geometry of Ref.[30]. It was this that was taken subsequently as the basic geometry in the search for the neutron optical potential parameters for ^{51}V.

The procedure for the optical potential parameter search was carried out in several steps. In the first, the neutron potential parameters for E_n = 100 keV were determined. The evaluated values of the S-neutron strength function and also the potential scattering radius R' [17] served as experimental data. Their values with errors are given in Fig. 1 and Table 1. In order to describe simultaneously the experimental values of the strength

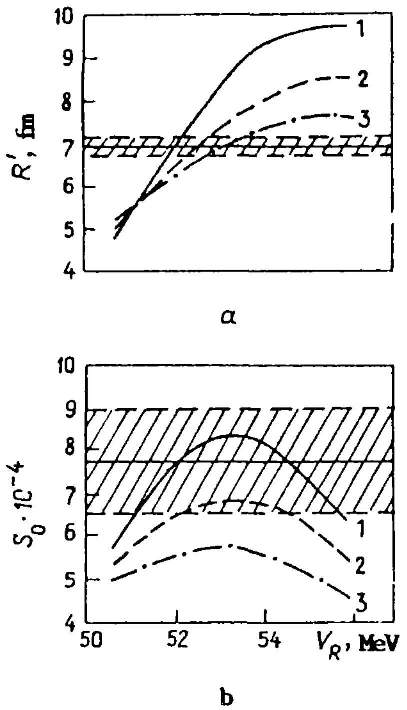

Table 1. Strength functions of S- and p-neutrons and the potential scattering radius for ^{51}V calculated at different values of potential depth (W_d = 3 MeV)

Evaluation and calculation	$S_0 \cdot 10^4$	$S_1 \cdot 10^4$	R', fm
Evaluation /18/	7,7±1,2	-	6,9±0,2
Calculation for V_R equal to (MeV):			
51	6,28	0,50	5,31
52	7,60	0,46	6,81
53	8,27	0,43	8,24

Fig. 1. Influence of changes in the optical potential parameters on the calculation of the potential scattering radius (a) and the strength function of s-neutrons (b) of the ^{51}V nucleus. Curves 1-3 represent the values of parameter W_d equal to 3, 4, 5 MeV respectively. The evaluated data on R and S_0 [17] are shown by continuous horizontal lines and their error by the hatched region.

function and the potential scattering radius, we have to choose the values of V_R = 52 MeV and W_d = 3 MeV (see Fig.1).

In the second step, on the assumption of a reasonable energy dependence of the potential depths, the neutron potential is determined within the low-energy interval of the total neutron cross-sections. For the ^{51}V nucleus the situation in this case is complex since the experimental data [19, 20] in the interval up to 1 MeV oscillates from 1 to 6.5 b and in the 1-2 MeV region from 2.5 to 4.5 b. In order to get the trend in the behaviour of the experimental values of σ_t, we averaged them over the range of 25 keV (Fig. 2) and 100 keV (Fig. 3). It will be seen from Fig. 2 that a 2% change in the optical potential depth leads to a 10% change, on an average, in the total cross-section at neutron energies of about 0.4 MeV. By averaging the experimental data in this sector of the spectrum over the 25 keV range it is not possible, as before, to obtain the trend in the energy dependence of the total neutron cross-sections. The situation is improved during the analysis of the total cross-section in a wider energy region and with averaging over the 100 keV range (see Fig. 3).

As a result of the procedure described above, we obtained the following set of neutron optical potential parameters for ^{51}V, which ensures a good

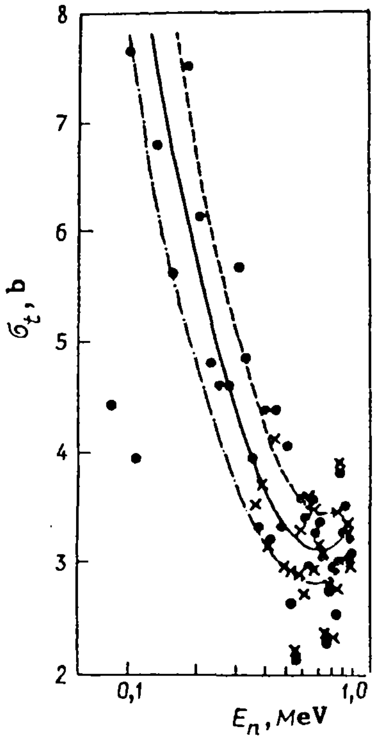

Fig. 2. The sensitivity of the calculated cross-sections σ_t of the ^{51}V nucleus to changes in the potential depth V_R for W_d = 3 MeV.

•, × - represent the experimental data of Refs [19, 20], respectively (averaged over the 25 keV range). The curves were calculated for V_R, MeV: — · —51; ——52; - - - - 53.

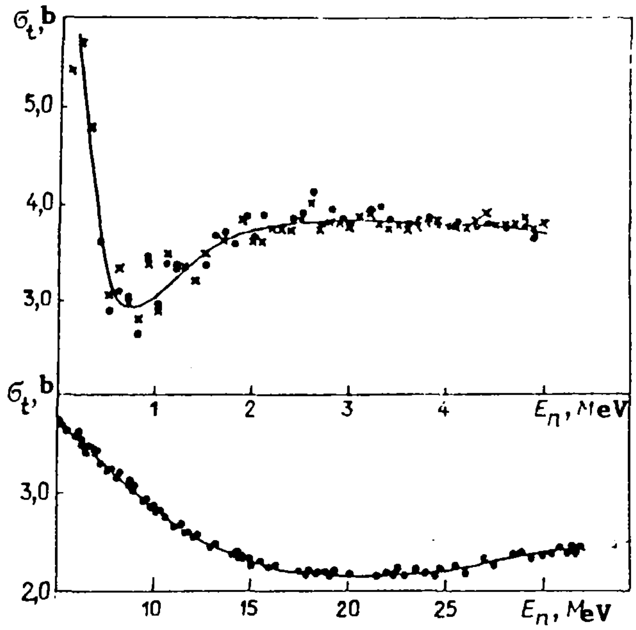

Fig. 3. The experimental data (•,x correspond to Refs [19, 20] and the results of calculation with optical potential (14) of the total neutron cross-sections for ^{51}V. The experimental data in the region up to 5 MeV (top) are averaged over the 100 keV range.

self-consistent reproduction of all the available experimental data in the region up to 32 MeV:

$$V_R = \begin{cases} 52 - 0{,}5E & (E \leq 8\ \text{MeV}), \\ 50{,}64 - 0{,}33E & (E \geq 8\ \text{MeV}); \end{cases} \quad r_R = 1{,}198;\ a_R = 0{,}663;\ V_{SO} = 6{,}2;\ r_{SO} = 1{,}01;\ a_{SO} = 0{,}75;$$

$$W_v = \begin{cases} 0 & (E \leq 15\ \text{MeV}), \\ -1{,}5 + 0{,}1E & (E > 15\ \text{MeV}); \end{cases} \quad W_d = \begin{cases} 3 + 1{,}38E & (E \leq 2\ \text{MeV}); \\ 5{,}76 & (2 \leq E \leq 8\ \text{MeV}); \\ 6{,}64 - 0{,}11E & (E > 8\ \text{MeV}); \end{cases} \quad r_d = r_v = 1{,}295;\ a_d = a_v = 0{,}588, \tag{14}$$

where all the dynamic parameters are given in megaelectron-volts and the geometrical parameters in femtometres.

Figure 4 shows the values of volume integrals per nucleon calculated with the set of paramters (14), together with calculations using the well-known global systematics of the optical potential. One should note the low value and the strong energy dependence of the imaginary component of the optical potential in the region up to 2 MeV. Only in this manner is it

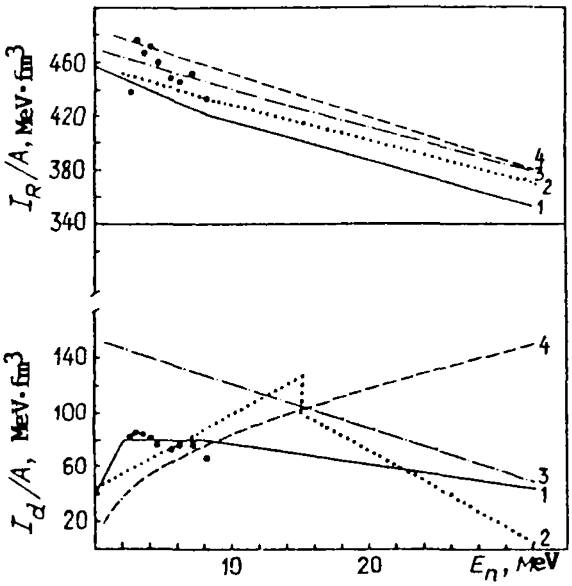

Fig. 4. The energy dependence of I_R/A and I_d/A for different sets of optical potential parameters: 1 – (14); 2 – [30]; 3 – [29]; 4 – [31]; • – caluclation with the optical potential parameters from Ref. [18].

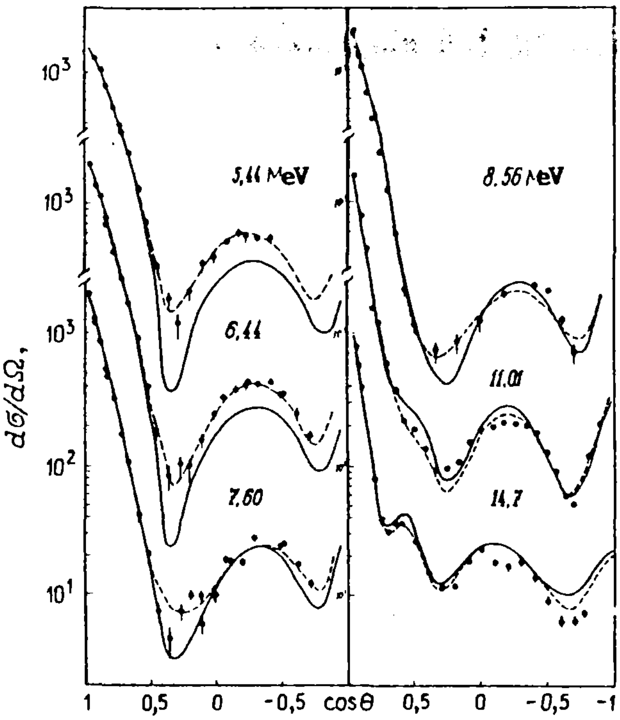

Fig. 5. Comparison with experiment [21–23] of the differential elastic scattering cross-sections for 5.44–14.7 MeV neutrons on the ^{51}V nucleus. The curves are calculated with the optical potential on the basis of: ——— expressions (14); – – – – Table 2.

possible to describe the observed irregularities of the neutron cross-sections in the low-energy part of the spectrum.

The set of parameters (14) of the neutron optical potential was also used to calculate the angular distributions of neutron elastic scattering in the energy region where the contribution of the compound nucleus mechanism can be neglected. The comparison between calculations and experimental data is shown in Fig. 5. Here, too, are given the calculations with the individual optical potential sets obtained for each energy of the scattered neutron by automatic search for them from the experimental differential cross-sections. Using the χ^2-criterion (8), we varied four optical potential parameters: V_R, τ_R, W_d, τ_d, for fixed values of the remaining parameters from set (14). The final results of this individual fitting, together with the other parameters, are given in Table 2.

On the basis of these calculation results we can draw the following conclusions. For the neutron optical potential set (14) obtained by matching potentials with different energy dependences of depths we can, on an average, satisfactorily describe the whole set of experimental data on neutron

Table 2. Individual sets of the neutron optical potential parameters for ^{51}V in the neutron energy region of 5.44-14.7 MeV.

Parameter	5,44	6,44	7,60	8,56	II,0I	I4,7
V_R, MeV	57,26	48,20	4I,83	45,67	49,63	55,47
r_R, fm	I,I2	I,22	I,29	I,25	I,I7	I,09
W_d, MeV	4,45	4,I6	6,I6	6,34	6,2I	6,58
r_d, fm	I,I9	I,35	I,I2	I,I4	I,24	I,20
χ^2	0,30	I,85	3,34	I,42	I7,9	9,2I
σ_t, b	3,47	3,66	3,36	3,I7	2,69	2,28
σ_t^{exp}, b	3,60	3,42	3,22	3,08	2,63	2,30
I_R/A, MeV·fm^3	426	44I	45I	449	4I0	383
I_d/A, MeV·fm^3	53	63	65	70	80	79
$\langle r_R^2 \rangle^{1/2}$	4,06	4,28	4,46	4,36	4,I7	3,99
$\langle r_d^2 \rangle^{1/2}$	5,0I	5,53	4,78	4,86	5,I9	5,04

scattering on ^{51}V in the 10 keV-32 MeV region. A distinguishing feature of set (14) is the considerably stronger energy dependence of its dynamic parameters in the low-energy part of the spectrum than in the high-energy part.

The anomalously strong energy dependence of the optical potential parameters at low energies (below 3 MeV) of scattered neutron on nuclei in the A ≈ 40-80 range is discussed in many studies [32, 33]. Clearly pronounced irregularities can occur in the behaviour of the optical potential parameters for ^{51}V in the above-mentioned kinematic range for several reasons.

First of all, in the low-energy region of the spectrum the basic condition of applicability of the optical model may not be fulfilled, namely the requirement that in the reaction many compound states should be excited whose averaging smooths out the singularities of the nucleus considered [27]. If the energy spread of the scattered particles is substantially greater than the average distance between the compound nucleus levels, these requirements are almost always fulfilled and the optical model is applicable. But this is not obvious beforehand in the case of the scattering of neutrons of an energy lower than 3 MeV on ^{51}V, whose level density is low.

Secondly, in this kinematic range the influence of the initial states on the formation of the observed distributions can be appreciable. Here, too, the effects of closed channels and near-threshold phenomena can be considerable.

Thirdly, at low energies of neutron scattering on nuclei with A ≈ 40-60 there is a high probability for the effects of collectivesingle particle fragmentation to appear and this can also affect the formation of the imaginary part of the optical potential [32].

The parameters of the isovector component of the nucleon optical potential

In the next step of the search for the nucleon optical potential parameters we analysed the experimental data on the $^{51}V(p,n)^{51}Cr(IAS)$ reaction in the 17.7-40 MeV proton energy range. The following procedure was set up to search for the parameters of the isovector component of the optical potential. It was assumed that in quasi-elastic scattering the form factor of interaction was determined by the real volume-component and the imaginary surface component. The geometrical parameters of the neutron potential were taken as the basis of the proton potential and the form factor of interaction. The isoscalar component of the nucleon potential was formed on the basis of the starting values of parameters V_1^R and W_1^d of the isovector component and on that of the neutron optical potential (14). The proton optical potential parameters were then obtained in accordance with definition (3). Thereafter the quasi-elastic proton scattering cross-sections for ^{51}V were calculated by the VAR-82 program [26] taking into account relations (9)-(13). The angular and integral charge exchange characteristics calculated for different energies of scattered protons were compared with the available experimental data [8, 9]. The initial values of V_1^R and W_1^d were then varied and the calculations repeated again. We thus determined the sensitivity of the angular and integral cross-sections in the $^{51}V(p,n)^{51}Cr(IAS)$ reactions to changes in the dynamic components of the isovector potential. Moreover, for each energy of the scattered proton we found the individual sets of parameters of the isovector component which describe the experimental data best. The final results of this iteration procedure are given in Table 3 and Fig. 6.

The following conclusions can be drawn from an analysis of the results obtained. It is observed that there is an explicit dependence of the parameters of the isovector component on the scattered proton energy - V_1^R and W_1^d decrease with increase in E_p. The same trend of change in the isovector component with increase of proton energy was found also in other studies [12, 14] on quasi-elastic scattering on the basis of the systematics of Bechetti and Greenlees. What is new in our results is that the anomalous behaviour of the integral cross-sections in the threshold region of the (p,n)(IAS) reaction can essentially be explained on the basis of the

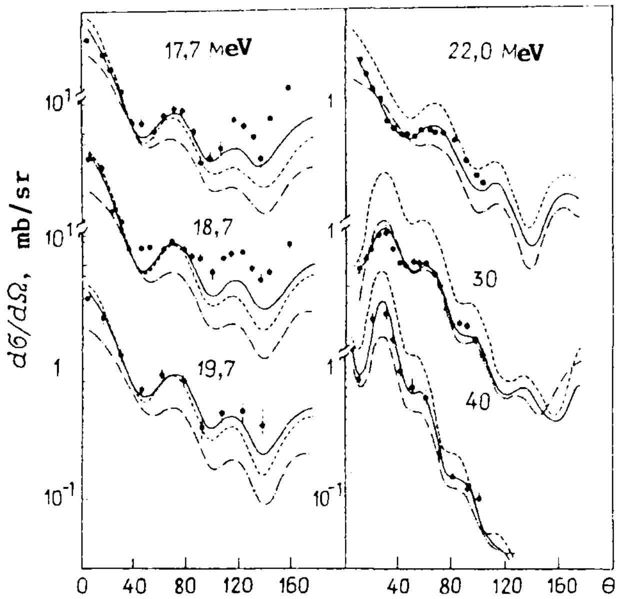

Fig. 6. The differential cross-sections for the $^{51}V(p,n)^{51}Cr$ (IAS) reaction at proton energies from 17.7 to 40 MeV: • – experimental data [8, 9]; – – – calculation on the basis of the proton and neutron global systematics of Bechetti and Greenlees [29]; —· —· —·and ——— calculation by the self-consistent Lane model with the potential of Ref. [30] and (14), and Table 3, respectively.

Table 3. Integral cross-sections of the $^{51}V(p,n)^{51}Cr$ (IAS) reaction calculated with different optical potential sets, mb

Parameters	Proton energy, MeV					
	I7,7	I8,7	I9,7	22,0	26,0	30,0
σ^{exp}_{pn} [8]	I0,0	9,4	8,I	7,4	6,3	-
σ^{T}_{pn} [29]	7,40	7,47	7,53	7,64	7,79	8,04
σ^{T}_{pn} [30]	5,3I	5,03	4,77	4,I8	3,83	3,70
σ^{T}_{pn}, Present study	9,50	9,2I	8,6I	7,30	6,52	6,08
V^{R}_{1}, "	I6,62	I4,3I	I4,2I	I2,5	I0,37	8,9I
W^{d}_{1}, "	II,83	I0,06	I0,0	7,3I	6,2I	6,0I

Remarks. The last two lines give the values of the parameters of the optical potential isovector component that best describe the experiment with main potential (14). The calculated (T) and experimental (exp) cross-sections are given in millibarns and V^{R}_{1} and W^{d}_{1} in megaelectron-volts.

neutron optical potential (14) and the consequent self-consistent approach of Lane.

The final search for the nucleon optical potential parameters for ^{51}V does not end with the analysis of quasi-elastic scattering data. It is very important to find such an optimal set of optical potential parameters as would self-consistently describe the totality of all accessible experimental data on neutron and proton scattering in a wide energy interval. For this purpose, it is necessary to determine the parameters of the isovector component at energies below the threshold of the $^{51}V(p,n)^{51}Cr$(IAS) reaction ($Q = 8.146$ MeV) and to describe the observed distributions over nucleon elastic and inelastic scattering in the sub-Coulomb region of energies, where an appreciable contribution to the cross-section is made by the process of scattering with compound nucleus formation. However, this complex situation requires a careful study [34].

REFERENCES

[24] TITARENKO, N.N., "A program set for calculation of two-particle reaction cross-sections" in: Neutron Physics (Proceedings of the Sixth All-Union Conference on Neutron Physics, Kiev, 2-6 October 1983) 1, TsNIIatominform, Moscow (1984) 116-120 (in Russian).

[25] TITARENKO, N.N., ROM-78 Program. Calculation of Elastic Scattering Cross-sections for Particles on Atomic Nuclei Using the Optical Model. Report FEhI-1230, Obninsk (1981) (in Russian).

[26] TITARENKO, N.N., VAR-82 Program. Calculation of Nuclear Reaction Cross-sections by the Distorted Wave Method. I. General Description. Collective Models. Report FEhI-1331, Obninsk (1982) (in Russian).

[27] HODGSON, P.E., The Optical Model of Elastic Scattering, Atomizdat, Moscow (1966) (Russian translation).

[28] ABRAMOVITS, M.A., STIGAN, N., A Handbook of Special Functions with Formulae, Graphs and Tables, Nauka, Moscow (1979) (in Russian).

[32] FEDOROV, M.N., "The problems of optical-statistical description of neutron cross-sections for spherical nuclei at low and medium energies" in: Neutron Physics (Proceedings of the Sixth All-Union Conference on Neutron Physics, Kiev, 2-6 October 1983) 3, TsNIIatominform, Moscow (1984) 129-133 (in Russian).

[33] EFROSININ, V.P., MUSAELYAN, R.M., POPOV, V.I., "The intermediate structure of elastic scattering cross-sections for low-energy neutrons in the A = 70-8 region", Yad. Fiz. 29, 3 (1979) 631-643.

[34] ROMANOVSKIJ, E.A., "The proton optical potential for ^{51}V at near-barrier energies", ibid. 41, 3 (1985) 607-616.

Bibliographic index of studies included in the present issue in CINDA

Element S	Element A	Quan-tity	Labo ratory	Work-type	Energy (eV) min	Energy (eV) max	Page	Comments
PT	182	FRS	DUB	THEO	+7		49	ADEEV + MASS-E-DISTR OF FRAG, GRPH, CFD
PT	194	FRS	DUB	THEO	+7		49	ADEEV + MASS-E-DISTR OF FRAG, GRPH, CFD
PO	211	NF	FEI	THEO	+6	7.0+7	45	OSTAPENKO + FISS YLD VS E, GRPH, CFD
U	234	NFY	LIN	REVW	+6	+7	24	GUSEV + YLD LI,BE,CALC CDF EXPT, GRPH
U	235	FRS	DUB	THEO	-2	+7	49	ADEEV + MASS-E-DISTR OF FRAG, GRPH, CFD
U	235	FRS	KFK	REVW	2.5 -2		3	HASSE. MASS-E-DISTR OF FRAG, GRPH, CFD
U	236	FRS	LIN	REVW	+6	+7	24	GUSEV + E-DIST OF FRAG, H3, HE4, HE6, TBL
PU	239	NFY	LIN	REVW	-2		24	GUSEV + E-DISTR OF H3, HE4, HE6, GRPH
PU	240	FRS	LIN	REVW	+6	+7	24	GUSEV + E-DIST OF FRAG, H3, HE4, HE6, TBL
AM	243	NEY	LIN	REVW	+6	+7	24	GUSEV + YLD LI, BE, CALC CFD EXPT, GRPH
CM	245	FRS	KFK	REVW	2.5 -2		3	HASSE. MASS-E-DISTR OF FRAG, GRPH, CFD
CF	249	FRS	KFK	REVW	2.5 -2		3	HASSE. MASS-E-DISTR OF FRAG, GRPH, CFD
CF	252	FRS	KFK	REVW	SPON		3	HASSE. MASS-E-DISTR OF FRAG, GRPH, CFD
CF	252	FRS	DUB	THEO	SPON		49	ADEEV + MASS-E-DISTR OF FRAG, GRPH, CFD
CF	252	FRS	LIN	REVW	SPON		24	GUSEV + E-DIST OF FRAG, H3, HE4, HE6, TBL
MANY		FRS	FEI	REVW	+7		33	ITKIS + MASS-E-DISTR OF FRAG, GRPH, CFD